ISSN 1392–1207. MECHANIKA. 2019 Volume 25(3): 248–254

Research of Normal Contact Stiffness of Straddle-Type Monorail Tyres Based on Fractal Theory

Zixue DU*, Junchao ZHOU, Xiaoxia WEN*****
**Institute of Urban Rail,Chongqing Jiaotong University, Chong Qing 400074,PR.China, PR.China,*
E-mail: aaadzx@163.com.
***Institute of Urban Rail,Chongqing Jiaotong University, Chong Qing 400074,PR.China, PR.China,*
E-mail: zhou1987g@163.com
School of Mechanical Engineering and Sichuan Provincial Key Lab of Process Equipment and Control, Sichuan University of Science and Engineering, Zigong, Sichuan ,643000
****Institute of Urban Rail, Chongqing Jiaotong University, Chong Qing 400074, PR, China, E-mail: 21930315@qq.com*
crossref http://dx.doi.org/10.5755/j01.mech.25.3.22265

1. Introduction

With the development of big cities, traffic congestion caused by vehicles has become a negative factor that impacts people's quality of life [1].To reduce traffic congestion, urban monorail vehicles especially straddle monorail vehicles have gained the attention of many researchers. The travelling system of a straddle-type monorail vehicle consists of the running tires, the guide tires and the bogies. A tubeless radial tire filled with nitrogen is used as the running tire. The performance of tyre has influences on dynamics of straddle-type monorail vehicles as well as the service life of tyres [2]. It is urgent to perfect theories and methods for selection of the surface roughness parameter of tread interaction as well as loads of tyres. As a result, the research on the contact stiffness of the tread interaction roughness surface of straddle-type monorail vehicles plays theoretical and practical roles. However, there is no sufficient theoretical support for the normal contact stiffness of straddle-type monorail vehicles tread interaction.

The contact parameter on the junction surface, especially the contact stiffness, has been a hot spot for related investigations in recent years at home and abroad. R. Buczkowski etc. used the fractal theory based on a single variable Weierstrass–Mandelbrot function to obtain the normal contact stiffness, taking into account the actual deformation of asperities and a correction [3].The reference [4] described a theoretical model that predicted the interfacial contact stiffness of fractal rough surfaces by considering the effects of elastic and plastic deformations of the fractal asperities. The fractal character of the stone surfaces was established to account for the contribution to rubber friction of stone roughness at different length scales and show that this method can be used to quantify the friction coefficient of sliding rubber as a function of surface roughness, load, and speed [5].P. Liu etc. proposed a modified fractal model for normal contact stiffness considering friction by the simulation [6]. The effects of surface roughness and fractality on the normal contact stiffness were experimentally demonstrated for various rough surfaces [7]. The sphere- and cylinder-based fractal bodies in contact with a smooth and rigid flat surface was discussed [8]and A revised elastic–plastic contact model of a single fractal asperity was also proposed [9]. The fractal model to calculate normal contact stiffness (NCS) for spheroidal contact bodies considering friction factor in order to calculate NCS was discussed [10]. J. Liao etc. proposed a method to identify the contact behaviors of shrink-fit toolholder joint and the contact stiffness model for the joint was established based on fractal geometry theory [11]. The above literatures involve in the three-dimensional analogue simulation software and the other one is parameter estimation based on the fractal theory. However, the methods have the following disadvantages: firstly, they lay emphasis on contact substance homogeneity, but not heterogeneity. Secondly, they mainly take contact between metals as the research object, but not between metal and nonmetal as well as between nonmetals. The contact parameter between tire and rail surface is a new field.

In addition, some other scholars have researched the contact stiffness between tires and tracks. D. Wang, A etc. [12] reported on an extensive study of the perpendicular stiffness between a rubber block and different road surface, and obtain good correlation between measured and calculated stiffness values by the theory—the elastic contact stiffness of a junction was determined by the surface roughness power spectrum of the surfaces. The dynamic behavior of straddle-type monorail tracks were discussed through wheel-track contact [13, 14]. But there is little discussion about contact stiffness between tire and rail.

In general, there are two main research methods for contact stiffness of junction surfaces: the first one is the three-dimensional analogue simulation software and the second one is the parameter estimation based on the fractal theory. However, the methods have the following disadvantages: Firstly, the emphasis is often laid on contact substance homogeneity, but not heterogeneity. Secondly, contact between metals is often taken as the research objective, but not between metal and nonmetal as well as between nonmetals. Considering that it is difficult to process surfaces with specific fractal parameters and there is no uniform methods utilized for the actual surface fractal parameters, the simulation or non-experimental verification is often adopted in practice; i.e., too much attention is paid to theory but not experiment. Therefore, related research works have been developed [7]. However, the lack of effective verification is still the barrier for the integration between theory and practice in researches on contact stiffness, and less breakthrough or progress has been made so far.

Therefore, analysis on normal contact stiffness on junction surfaces between tyres and tracks of straddle-type

monorail vehicles is conducted macroscopically and microscopically. There are two achievements: 1.an innovative model for the normal stiffness of tread interaction is proposed. The establishment of the model provides theoretical basis for the tire-track contact dynamics. 2. the model macroscopically in ways of simulation is verified by physical experiments.

This article is organized as follows: In the first part, the rubber tread interaction normal stiffness model is established based on the fractal theory and the Hertz contact theory; In the second part, the influences on the normal contact stiffness of various factors of the system are comprehensively analyzed, including the shape of tire surface, the material of tyres and loads; Last but not least, experimental analysis is conducted with numerical simulation and physical experiments.

2. Fractal model of the contact stiffness on the tread interaction surface

The tread interaction surface is rough in microscale, and the surface profile curve of the face has self-affinity fractal feature on statistics, which is irrelevant to scales[12]. Based on the following assumption that the microstructure on the rough surface has isotropy; the interaction between various micro-bulges on the rough surface can be ignored. The junction surface is actually composed by two rough surfaces, which can be regarded as a sphere for any micro-bulge.

Majumdar and Bhushan proposed elastic-plasticity M-B fractal contact model based on W-M fractal function. According to the literature [15, 16], in the amended M-B fractal contact model, in condition of contact between the fractal rough surface and the ideal stiffness plane, the contact distribution function of the micro-bulge is listed as follows:

$$\begin{cases} n(A)=\dfrac{D}{2}\psi^{(2-D)/2}A_l^{D/2}A^{-(D+2)/2}, \\ \dfrac{\psi^{(2-D)/2}-\left(1+\psi^{-D/2}\right)^{-(2-D)/D}}{(2-D)/D}=1, \\ A_r=\int_0^{A_l} n(A)AdA=\dfrac{D}{2-D}\psi^{(2-D)/2}A_l. \end{cases} \tag{1}$$

In which, D is the fractal dimension, and ψ is the expanding coefficient of the fractal region; A is the contact area of the micro-bulge; A_l is the maximum contact area of the single-point micro-bulge; A_r is the actual contact area of the contact surface.

According to the Hertz contact theory, δ_c, the critical point deformation of the elastic deformation of the micro-bulge can be expressed as follows:

$$\delta_c=\left(\frac{P_m}{2E}\right)^2\frac{A^{D/2}}{G^{D-1}}, \tag{2}$$

In which, P_m is the maximum contact pressure of the material, and E is the composite elastic modulus.G is a scale factor.

$$\frac{1}{E}=\frac{1-\mu_1^2}{E_1}+\frac{1-\mu_2^2}{E_2}. \tag{3}$$

In which, E_1, E_2 and μ_1, μ_2 are elastic modulus and poisson ratio of materials of the two contact surfaces. Solve Eqs. (2) and (3) together, to acquire A_c, the contact area in the critical state:

$$A_c=G^2\left(\frac{2E}{P_m}\right)^{2/D-1}. \tag{4}$$

According to the definition of stiffness [17]:

$$k_n=2E\left(\frac{A}{\pi}\right)^{1/2}. \tag{5}$$

The overall junction surface contact stiffness is illustrated as follows:

$$\begin{aligned} K_n&=\int_{A_c}^{A_l}k_n n(A)dA= \\ &=\int_{A_c}^{A_l}2E\left(\frac{A}{\pi}\right)^{1/2}\frac{D}{2}\psi^{(2-D)/2}\left(A_l\right)^{D/2}(A)^{-(D+2)/2}dA. \end{aligned} \tag{6}$$

After arrangement:

$$K_n=\frac{2ED}{\sqrt{\pi}(1-D)}\psi^{(2-D)/2}A_l^{D/2}\left[A_l^{(1-D)/2}-A_c^{(1-D)/2}\right]. \tag{7}$$

Conduct non-dimensionalization to Eq. (7), to acquire the dimensionless normal contact stiffness:

$$\begin{aligned} K_n^*&=\frac{2D}{\sqrt{\pi}(1-D)}\phi^{\frac{1-D}{2}}\left(\frac{2-D}{2}\right)^2A_r^{*\frac{D}{2}}\times \\ &\times\left[\left(\frac{2-D}{D\phi}\right)^{\frac{1-D}{2}}\phi^{\frac{-D^2+3D-2}{4}}A_r^*-A_c^{*\frac{1-D}{2}}\right]. \end{aligned} \tag{8}$$

in which:

$$K_n^*=K_n/E\sqrt{\pi}, A_r^*=A_r/A_a, A_c^*=\frac{A_c}{A_a}=\frac{G^{*2}}{(k\phi/2)^{\frac{2}{D-1}}},$$

A_a is the nominal contact area; A_r^* is the dimensionless actual contact area; A_r is the actual contact area; A_c^* is the dimensionless critical contact area.

Eq. (8) includes various factors such as the fractal dimension D of the microstructure of the tread interaction surface, the fractal scale parameter G^* and the macroscopic size factor A_r.

According to the literature [11], the relationship between A_e, the sectional area of the elastic contact point, and p_e, the normal elastic contact load, is:

$$p_e(A_e)=\frac{\sqrt{2}\pi}{3}EG^{(D-1)}A_e^{\frac{3-D}{2}}. \tag{9}$$

The relationship between A_p, the upper disconnection area of the plastic contact point, and p_p, the normal plastic contact load, is in the reference [6]:

$$p_p\left(A_p\right)=\frac{1}{2}k\sigma_y A_p, \tag{10}$$

in which: $k=H/\sigma_y$, and H is the stiffness of the softer material, and σ_y is the yield strength of the softer material.

Therefore, the relationship between the total normal load P and the actual contact area on the junction surface is:

$$P=p_e+p_p=\frac{\sqrt{2}\pi EG^{(D-1)}}{3}\times \times\int_{A_c}^{A_l} n(A)A^{(3-D)/2}dA+\frac{1}{2}k\sigma_y\int_0^{A_c} n(A)AdA. \tag{11}$$

After the introduction of the amendment, the relationship between the normal load and the contact area on the junction surface is listed as follows:

1. If $A_l > A_c$, and there is elastic deformation on the contact point.The dimensionless total normal load on the junction surface [11] is:

$$\begin{cases} P^*=\dfrac{4\sqrt{\pi}}{3}G^{*(D-1)}g_1(D)\phi^{\frac{(D-2)^2}{4}}A_r^{*\frac{D}{2}}\times\left[\left(\dfrac{(2-D)\phi^{\frac{(D-2)}{2}}A_r^*}{D}\right)^{\frac{(3-2D)}{2}}-A_c^{*\frac{(3-2D)}{2}}\right]+k\phi g_2(D)\psi^{\frac{(D-2)^2}{4}}A_r^{*\frac{D}{2}}A_c^{*\frac{2-D}{2}} & (D\neq 1.5) \\ P^*=3^{-\frac{3}{4}}\sqrt{\pi}G^{*\frac{1}{2}}\Psi^{\frac{1}{16}}A_r^{*\frac{3}{4}}\times ln\left(\dfrac{A_r^*}{3\psi^{\frac{1}{4}}A_c^*}\right)+3^{\frac{1}{4}}k\phi\psi^{\frac{1}{16}}A_r^{*\frac{3}{4}}A_c^{*\frac{1}{4}} & (D=1.5) \end{cases}, \tag{12}$$

in which: P^* is the load after dimensional normalization, and $P^*=\dfrac{P}{EA_a}$; G^* is the characteristic scale coefficient after dimensional normalization, and $G^*=\dfrac{G}{\sqrt{A_a}}$; ψ is the characteristic parameterof the contact body material, and $\phi=\dfrac{\sigma_y}{E}g_2(D)$; g_2 D is the function related to fractal dimension, with the following calculation formula:

$$g_1(D)=\frac{D}{3-2D}\left(\frac{2-D}{D}\right)^{\frac{D}{2}},g_2(D)=\left(\frac{D}{2-D}\right)^{\frac{1-D}{2}}. \tag{13}$$

2. If $A_l < A_c$, the contact points are at plastic contact, the total load in this condition is:

$$P^*=k\phi A_r^*. \tag{14}$$

3.Prediction on fractal model of tire contact stiffness

The fractal model of tire contact stiffness is established based on the Eqs. (8)-(14), and the relationship between the normal contact stiffness K_n^* and the load P^* is established according to the actual contact area A_r^* on the junction surface, to conduct numerical simulation to the relationship with the normal contact stiffness K_n^*.

The relationship between normal contact stiffness K_n^* and load P^* is illustrated in Fig.1. According to Fig.1:

1. There is an almost linear relationship between normal contact stiffness and load. The normal contact load increases with the growth of the load. Because the actual normal plastic contact area increases with the surface load; i.e., the actual contact area of the micro-bulge increases, which increases the normal load ability. It increases the contact stiffness on the junction surface. 2. Larger fractal dimension leads to larger normal stiffness under the same load. It is because that the critical contact area A_c^* decrease, the dimensional contact point in the elastic contact increase which the real contact area A_r^* increase.

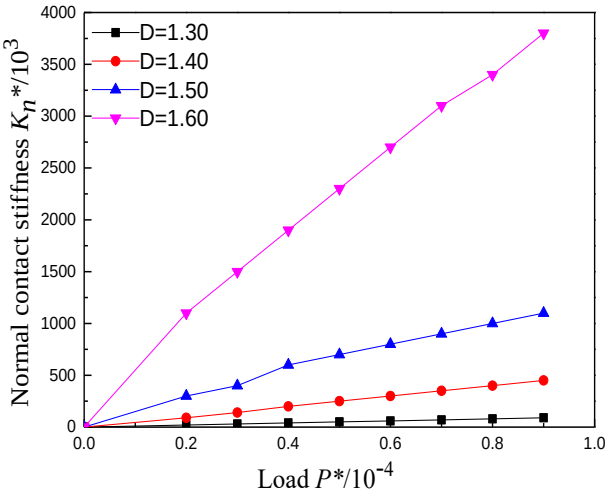

Fig. 1 Relationship curve between normal contact stiffness and load

If the load $P^*=1\times10^{-5}$, relationship curves between K_n^* and D under different G^* is illustrated in Fig .2. According to Fig.2: In condition of fixed load P* and characteristic scale G*, the contact stiffness on the junction surface increases with the growth of the fractal dimension. When the surface shape is close to a plane, i.e., D=2, the contact stiffness decreases. Therefore, there is an optimal value for the fractal dimension, which achieves the maximum tire normal stiffness.

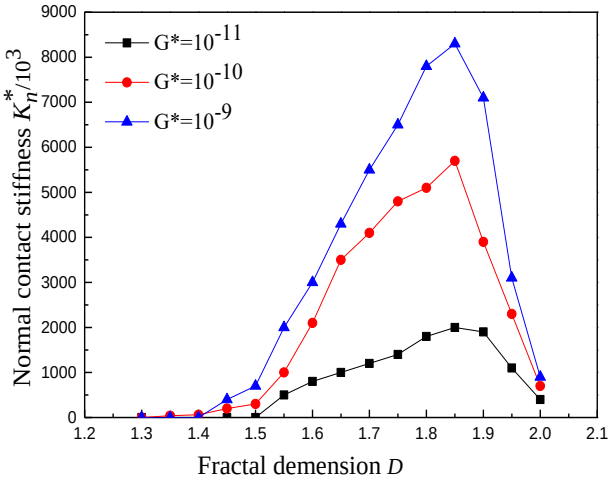

Fig. 2 Relationship between normal contact stiffness and fractal dimension

If the load is taken as $P^* = 1\times10^{-5}$, the changing curve of K_n^* with G^* under different D values can be acquired, as shown in Fig.3.

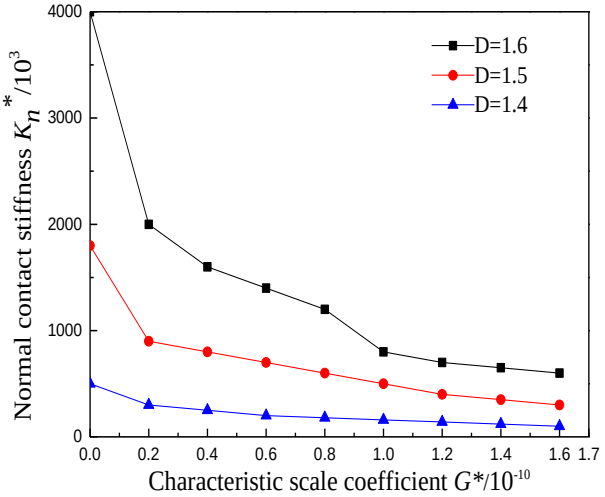

Fig. 3 Relationship between normal contact stiffness and characteristic scale coefficient

The relationship between normal contact stiffness K_n^* and characteristic scale coefficient G^* is illustrated in Fig .3. As shown in Fig .3:

1. for the same fractal dimension D, the normal contact stiffness K_n^* decreases with the growth in characteristic scale coefficient. Higher G^* indicates higher surface roughness, and the plastic contact point and the actual contact area A_r^* are reduced. It leads to the junction surfaces stiffness K_n^* decrease. According to Fig .3, the reduced roughness helps for the improvement on the normal stiffness of tire contact.

2.for the same characteristic scale coefficient, larger fractal dimension lead to larger normal stiffness K_n^* .Larger fractal dimension increases normal contact stiffness.

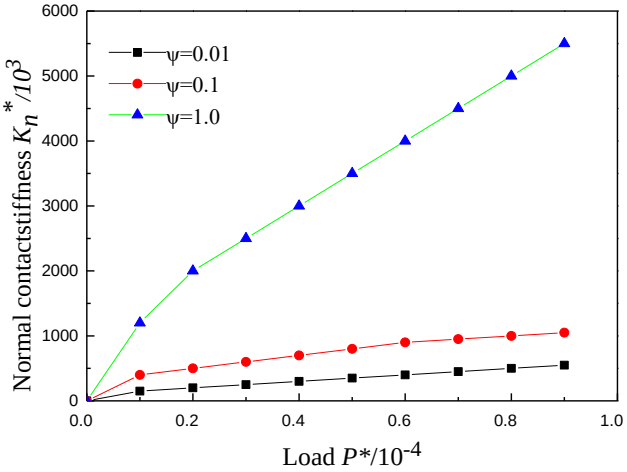

Fig. 4 Relationship between normal contact stiffness and material coefficient

If D=1.45 and k=1, the normal contact stiffness K_n^* with different φ is illustrated in Fig.4. According to Fig .4:

1. The normal contact stiffness K_n^* increases with the growth of load. This is consistent with the reference [6].

2.Under the same load, larger ψ indicates larger normal stiffness. Because larger ψ value indicates larger yield strength or smaller comprehensive elastic modulus of the material. It leads to stiffness on the junction surface increased.

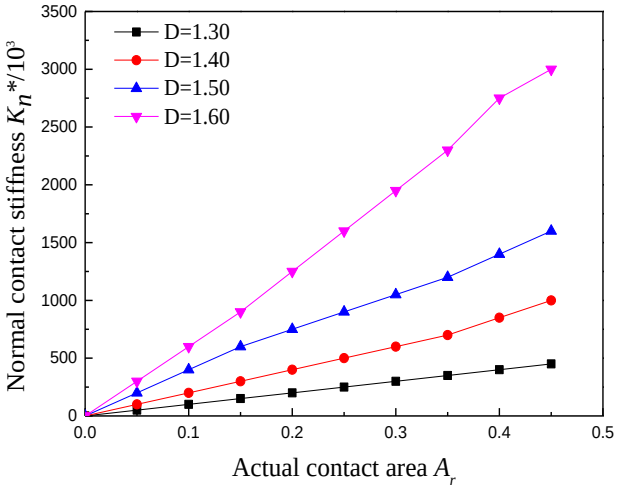

Fig. 5 Relationship between normal stiffness and actual contact area

The relationship between normal stiffness K_n^* and actual contact area A_r is illustrated in Fig.5. According to Fig .5:

1. The normal contact stiffness increases with the contact area. Because larger actual contact area indicates larger elastic contact deformation ratio and stronger elastic deformation ability stored on the contact surface. It leads to larger stiffness.

2. Under the same actual contact area, the normal stiffness increases with the growth of the fractal dimension.

4. Results and discussions

It is necessary to verify the contact stiffness of the theoretical contact model macroscopically by conducting the experimental method.

The deformation degree of the loaded running tires gives rise to direct influences on the trend interaction state and the stiffness. The experiment is conducted on the stiffness of the tyres to conduct finite element simulation to acquire actual forces and deformations on 3 directions. Finite element analysis is conduct on 4 groups of tyres of different loads, to calculate the normal stiffness of the junction surface of tyres by utilizing the fractal model. In the fractal model, the measured fractal dimension is 1.5, and the material coefficient is 0.1, and the characteristic scale coefficient is 1×10^{-10} , and the friction factor is 0.1 [15]. The geometrical profile of the running tyres and density parameters of various parts in the finite element analysis are provided by a Chinese tire manufacturer. In the finite software ABAQUS, the *re-bar* reinforcing bar units are adopted to simulate the wire cord fabric, and Mooney-Rivlin is adopted as the dynamic constitutive model of rubber materials [18]. Material parameters of PC track beam is illustrated in the Table 1[18].The rubber model body unit has 8 nodes, as a linear hexahedron hybrid entity unit (C3D8H). The four-node tetrahedron element is adopted for wire cord fabric (SFM3D4R). The mesh size is about 8mm and the model has 791 nodes and 655 elements in total. The friction coefficient of the tire-truck contact surface is zero at the static state. Then, the steady-state transmission method is used to transfer the analysis under static load to the steady-state rolling analysis. By combining the three-dimensional model of running tyres and the model of the track beam, the finite element model for tire-track contact is established the finite element model of tire-track contact is illustrated Fig. 6. The normal stiffness fractal theory and the finite results are as shown in Table 2. From Table 2, we can see that the error between normal stiffness fractal theory model and finite element result is about 10%, which is in the allowed range relative. This verifies the accuracy by finite element model.

Table 1

Material parameters of PC track beam

Material parameters	Density (kg/m3)	Elastic modulus (MPa)	Poisson ratio
PC track beam	2450	36000	0.2

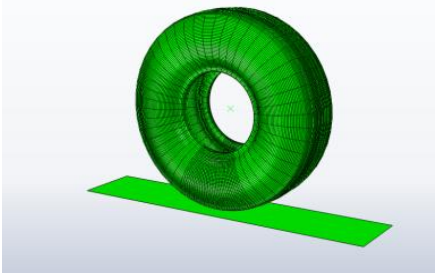

Fig. 6 Finite element model of tire-track contact

The contact surface on the normal junction surface is composed by two surfaces; i.e., tire surface and simulated turnout surface. Under certain junction surface pairing conditions, the normal load is implemented vertically in a hierarchical way. It is available to acquire the normal face pressure and the normal displacement through the pressure sensor and the eddy-current transducer, so as to acquire the relation between the static stiffness and the deformation or the load .

Table 2

Normal stiffness fractal theory model and finite element analysis result

Load/KN	15	30	45	60
Fractal model K_n^* /10^3	200	500	800	1196
Finite element analysis K_n^* /10^3	218	473	761	1280
Error%	9.00	5.40	7.30	7.02

Load from 0 kN to 60 kN in a speed of 15 kN/min along with the vertical direction of tyres, and record the force-displacement curve. Fix the running tire assembly to the experimental platform, and apply vertical pressure of 15 kN, 30 kN, 45 kN and 60 kN with the vertical preload actuator to running tyres. During the experiment, keep the vertical preload unchanged with simulated pavement material and friction coefficient the same as real roads. The simulated pavement is pushed and pulled by driving the actuator to collect the curve between the force driving the actuator and the displacement and calculate the normal stiffness of tyres. Please refer to Table 3 for experimental equipment and models. Four groups of different load experimental values are taken and the fractal model calculation method is utilized to calculate the normal stiffness for comparison, as illustrated in Table 4. The experimental process is illustrated in Fig .7. The MTS Hydraulic cylinder test system is designed. The tested tire is installed through the tire sliding rail. On the sliding rail. The counterforce hydraulic actuator, as the basis of the reaction force of tire forced vibration, works in the displacement control mode to keep the piston rod position unchanged.

According to Table 2 and Table 3, the curve between normal stiffness and load is acquired, as shown in Figure 8. According to Fig. 8, the calculation result of the fractal model of tyres is almost consistent with the finite element analysis and the experimental results, with experimental error within 10%. Under certain fractal dimension and material coefficient, the normal contact stiffness increases with the growth of loads.

Table 3

Experimental equipment and models

Materials	Models
Tires	335/90 R16,Inflatable pressure: 0.95Mpa ,Rated load: 5600kg
Sliding rails	Turnout concrete
Counterforce servo actuator	Hydraulic cylinder 1, MTS 244
Exciting servo actuator	Hydraulic cylinder 2, MTS 244

Table 4

Normal stiffness fractal theoretical models and experimental results

Load /kN	15	30	45	60
Fractal model K_n^*/10^3	200	500	800	1196
Experimental result K_n^*/10^3	187	526	741	1079
Error /%	6.50	5.20	7.38	9.78

Fig. 7 Experimental process

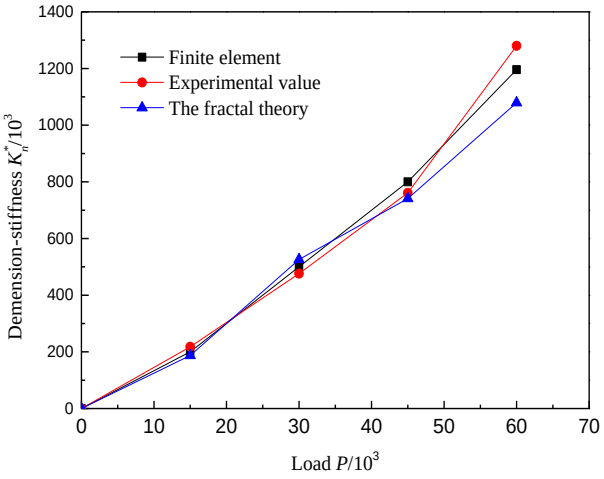

Fig. 8 Analysis on theoretical and experimental results

4. Conclusions

The theoretical model on normal contact of rubber tires of monorail vehicles is established microscopically. In addition, a systematic experimental procedure is established in details. The fractal model is analysed by simulation and physical test. The feasibility of proposed method is proved by the results. It provides a theoretical basis for the calculation of the contact stiffness of the tread interaction, and also provides a new method for the study of tire-track contact dynamics.

Acknowledgments

This work was supported by the National Natural Science Foundation of China (Grant No. 51475062) Talent Project of Sichuan University of Science and Engineering (Grant No.2017RCL42) and Project of Sichuan Provincial Department of Education (Grant No. 18ZB0423) and Sichuan Provincial Key Lab of Process Equipment and Control (Grant No. GK201806 and GK201707) and project of Zigong Science and Technology Bureau(2018YYJC14).

Reference

1. **MacIel, G. P. R.; Barbosa, R. S.** 2016. Monorail vehicle model to study influence of tyre modelling on overall dynamics, International Journal of Heavy Vehicle Systems 23(4):317-332. http://dx.doi.org/10.1504/IJHVS.2016.079270.
2. **Wen, X.-X.; Du, Z.-X.; Zhao, D.-Y.; Xu, Z.-Z.; Zhen, Y.** 2016. Study on the tire uneven wear mechanism of the running wheel of monorail vehicles, Journal of Applied Science and Engineering 19(4):459-470. http://dx.doi.org/10.6180/jase.2016.19.4.09.
3. **Buczkowski, R.; Kleiber, M.; Starzyński, G.** 2014. Normal contact stiffness of fractal rough surfaces, Archives of Mechanics 66(6):411-428. http://dx.doi.org/DOI: 10.1115/1.4006924.
4. **Zhang, D.; Xia, Y.; Scarpa, F.; Hong, J.; Ma, Y.** 2017. Interfacial contact stiffness of fractal rough surfaces, Sci. Rep. 7(1):12874. http://dx.doi.org/10.1038/s41598-017-13314-2.
5. **Villani, M.; Artamendi, I.; Kane, M.; Scarpas, A.** 2011. Contribution of Hysteresis Component of Tire Rubber Friction on Stone Surfaces, Transportation Research Record: Journal of the Transportation Research Board 2227(153-162. http://dx.doi.org/10.3141/2227-17.
6. **Liu, P.; Zhao, H.; Huang, K.; Chen, Q.** 2015. Research on normal contact stiffness of rough surface considering friction based on fractal theory, Applied Surface Science 349: 43-48. http://dx.doi.org/10.1016/j.apsusc.2015.04.174.
7. **Zhai, C.; Gan, Y.; Hanaor, D.; Proust, G.; Retraint, D.** 2015. The role of surface structure in normal contact stiffness, Experimental Mechanics 56(3):359-368. http://dx.doi.org/10.1007/s11340-015-0107-0.
8. **Liou, J. L.; Tsai, C. M.; Lin, J.-F.** 2010. A microcontact model developed for sphere- and cylinder-based fractal bodies in contact with a rigid flat surface, Wear 268(3-4):431-442. http://dx.doi.org/10.1016/j.wear.2009.08.033.
9. **Liou, J. L.; Lin, J. F.** 2010. A modified fractal microcontact model developed for asperity heights with variable morphology parameters, Wear 268(1-2):133-144. http://dx.doi.org/10.1016/j.wear.2009.07.003.
10. **Chen, Q.; Xu, F.; Liu, P.; Fan, H.** 2016. Research on fractal model of normal contact stiffness between two spheroidal joint surfaces considering friction factor, Tribology International 97:253-264. http://dx.doi.org/10.1016/j.triboint.2016.01.023.
11. **Liao, J.; Zhang, J.; Feng, P.; Yu, D.; Wu, Z.** 2016. Identification of contact stiffness of shrink-fit tool-holder joint based on fractal theory, The International Journal of Advanced Manufacturing Technology 90(5-8):2173-2184. http://dx.doi.org/10.1007/s00170-016-9506-3.
12. **Wang, D.; Ueckermann, A.; Schacht, A.; Oeser, M.; Steinauer, B.; Persson, B. N. J.** 2014. Tire–Road Contact Stiffness, Tribology Letters 56(2):397-402. http://dx.doi.org/10.1007/s11249-014-0417-x.
13. **Pu, Q.; Wang, H.; Gou, H.; Bao, Y.; Yan, M.** 2018. Fatigue behavior of prestressed concrete beam for straddle-type monorail tracks, Applied Sciences 8(7):1136. http://dx.doi.org/10.3390/app8071136.
14. **Hongye Gou, W. Z., Genda Chen, Yi Bao** and **Qianhui Pu**. 2018. In-situ test and dynamic response of a double-deck tied-arch bridge, Steel and Composite Structures 27(2):161-175. http://dx.doi.org/10.12989/scs.2018.27.2.161.

15. **Jiang, S.; Zheng, Y.; Zhu, H.** 2010. A contact stiffness model of machined plane joint based on fractal theory, Journal of Tribology 132(1):011401-011405. http://dx.doi.org/10.1115/1.4000305.
16. **Morag, Y.; Etsion, I.** 2007. Resolving the contradiction of asperities plastic to elastic mode transition in current contact models of fractal rough surfaces, Wear 262(5-6):624-629. http://dx.doi.org/10.1016/j.wear.2006.07.007.
17. **Shi, J.; Cao, X.; Zhu, H.** 2014. Tangential contact stiffness of rough cylindrical faying surfaces based on the fractal theory, Journal of Tribology 136(4):041401. http://dx.doi.org/10.1115/1.4028042.
18. **Du, Z.; Wen, X.; Zhao, D.; Xu, Z.; Chen, L.** 2017. Numerical Analysis of Partial Abrasion of the Straddle-type Monorail Vehicle running Tyre, Transactions of FAMENA, 41(1):99-112. http://dx.doi.org/10.21278/tof.41109.

ZX. Du, JC. Zhou, XX. Wen

RESEARCH OF NORMAL CONTACT STIFFNESS OF STRADDLE-TYPE MONORAIL TYRES BASED ON FRACTAL THEORY

S u m m a r y

The contact stiffness of on the rough surface of tread interaction (tire-track), a significant parameter for the tire-track contact surface, gives rise to direct influences on stiffness and noises of tyres. There is no sufficient theoretical support for the wheel face design due to lack of research on this parameter. To solve this problem, an innovative method based on the fractal theory and the Hertz contact theory is proposed to estimate tread interaction contact stiffness. The fractal theory model is established to research the influencing factors on normal contact stiffness on the tread surface. Finite element analysis and physical tests have been conducted to make comparisons about the model. According to research results, there is a non-linear relationship between the contact stiffness and the fractal dimension. The research provides theoretical basis for tyre dynamics of straddle-type monorail vehicles and design of the track contact dynamics.

Keywords: straddle-type monorail vehicles, tire-track beam, tire contact stiffness, fractal theory.

Received December 18, 2018
Accepted June 14, 2019